Neurobiology of Stress 33 (2024) 100687

Contents lists available at ScienceDirect

Neurobiology of Stress

journal homepage: www.elsevier.com/locate/ynstr

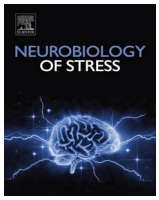

Prenatal exposures and cell type proportions are main drivers of *FKBP5* DNA methylation in maltreated and non-maltreated children

Vera N. Karlbauer [a,b], Jade Martins [a], Monika Rex-Haffner [a], Susann Sauer [a], Simone Roeh [a], Katja Dittrich [c], Peggy Doerr [c], Heiko Klawitter [d], Sonja Entringer [d,e,f], Claudia Buss [d,e,f], Sibylle M. Winter [c,e], Christine Heim [d,e,g,h], Darina Czamara [a], Elisabeth B. Binder [a,e,h,*]

[a] *Dept. Genes and Environment, Max Planck Institute of Psychiatry, Kraepelinstr. 2-10, 80804 Munich, Germany*
[b] *Graduate School of Systemic Neurosciences, Ludwig-Maximilians-Universität Munich, Germany*
[c] *Charité - Universitätsmedizin Berlin, Corporate Member of Freie Universität Berlin, Humboldt-Universität zu Berlin, Department of Child and Adolescent Psychiatry, Augustenburger Platz 1, 13353 Berlin, Germany*
[d] *Charité Universitätsmedizin Berlin, Corporate Member of Freie Universität Berlin, Humboldt-Universität zu Berlin, Institute of Medical Psychology, Campus Charité Mitte, Luisenstraße 57, 10117 Berlin, Germany*
[e] *Deutsches Zentrum für Psychische Gesundheit (DZPG), LMU Klinikum. Klinik für Psychiatrie und Psychotherapie, Nußbaumstr, 80336 München & Virchowweg 23, 10117 Berlin, Germany*
[f] *Development, Health and Disease Research Program, Department of Pediatrics, University of California Irvine, Irvine, USA*
[g] *Cluster of Excellence NeuroCure (EXC25), Charité Universitätsmedizin Berlin, Corporate Member of Freie Universität Berlin, Humboldt-Universität zu Berlin, Charitéplatz 1, 10117 Berlin, Germany*
[h] *Department of Psychiatry and Behavioral Sciences, Emory University School of Medicine, Atlanta, GA, 30329, USA*

ARTICLE INFO

Handling Editor: Dr. Tallie Z Baram

Keywords:
DNA methylation
Early-life adversity
Glucocorticoids
FKBP5
HAM-TBS

ABSTRACT

DNA methylation in peripheral tissues may be a relevant biomarker of risk for developing mental disorders after exposure to early life adversity. Genes involved in HPA axis regulation, such as *FKBP5*, might play a key role. In this study, we aimed to identify the main drivers of salivary *FKBP5* methylation in a cohort of 162 maltreated and non-maltreated children aged 3–5 years at two measurement timepoints. We combined data from a targeted bisulfite sequencing approach for fine-mapping 49 CpGs in regulatory regions of *FKBP5* and epigenetic scores for exposure to alcohol, cigarette smoke, and glucocorticoids derived from the EPICv1 microarray.

Most variability of methylation in the *FKBP5* locus was explained by estimated cell type proportions as well as epigenetic exposure scores, most prominently by the glucocorticoid exposure score. While not surviving correction for multiple testing, we replicated previously reported associations of *FKBP5* methylation with CM. We also detected synergistic effects of both rs1360780 genotype and the glucocorticoid exposure score on *FKBP5* hypomethylation. These effects were identified in the 3′TAD, a distal regulatory region of *FKBP5* which is not extensively covered in Illumina arrays, emphasizing the need for fine mapping approaches. Additionally, the epigenetic glucocorticoid exposure score was associated with childhood maltreatment, maternal mental disorders, and pregnancy complications, thereby highlighting the role of glucocorticoid signaling in the epigenetic consequences of early adversity.

These results underscore the need to assess cell type heterogeneity in targeted assessments of DNA methylation and show the impact of exposures beyond just childhood maltreatment such as glucocorticoid exposure.

1. Introduction

Exposure to childhood maltreatment (CM) has consistently been linked to an increased risk for developing psychiatric disorders later in life and epigenetic mechanisms have previously been proposed as means of the biological embedding of CM (Parade et al., 2021). Epigenetic changes are reversible changes on DNA and histones that are sensitive to environmental cues, including the social environment (Aristizabal et al., 2020).

The major neuroendocrine response to stress is the activation of the

* Corresponding author. Max Planck Institute of Psychiatry, Kraepelinstr. 2-10, 80804, Munich, Germany.
E-mail address: binder@psych.mpg.de (E.B. Binder).

https://doi.org/10.1016/j.ynstr.2024.100687
Received 12 August 2024; Received in revised form 22 October 2024; Accepted 4 November 2024
Available online 6 November 2024

hypothalamic pituitary adrenal axis (HPA axis) by stimulation of corticotropin releasing hormone and vasopressin from the paraventricular hypothalamus area, which leads to the stimulation of ACTH secretion in the pituitary and increases the secretion of glucocorticoids (GCs) from the adrenal cortex. Via the glucocorticoid receptor (GR), GCs are responsible for the termination of the axis activation through a negative feedback loop exerted on the central axis components. Therefore, increased exposure to GCs during stressful events, such as CM, has been proposed as one of the mechanisms of how early-life stressors can induce changes in DNA methylation (DNAm, Klengel et al., 2014). Due to their role in mediating and adapting the response to early stressors, the genes of the HPA axis have been considered central candidates to study epigenetic modifications following GC exposure induced by early life stressors such as CM (Jiang et al., 2019). One of these genes is *FKBP5*, which has been extensively studied in the context of gene-environment interactions and CM (Matosin et al., 2018; Normann and Buttenschøn, 2020).

The gene encodes the FK506 binding protein 51 (FKBP51) that serves as a negative regulator of GR function. GR activation induces *FKBP5* expression, thus providing an ultra-short feedback loop for GR sensitivity (Zannas et al., 2015). This activation is mediated by several glucocorticoid response elements (GREs), located across the locus, including in introns 2, 5, and 7.

DNAm changes in peripheral tissues (DNA from blood and saliva) have been reported for the *FKBP5* locus with exposure to adverse childhood experiences, both in children as well as adults (Matosin et al., 2018). Childhood adversity has been linked to decreased levels of DNAm at regulatory elements, especially in the context of genetic variations in *FKBP5* that have been associated with increased transcriptional response. For these genetic variants, gene-environment interactions have been reported, with mostly the combination of the alleles correlated with enhanced transcription and exposure to CM also being associated with increased risk for psychiatric disorders in a transdiagnostic way (Matosin et al., 2018). On rs1360780, the most commonly investigated single nucleotide polymorphism (SNP) on *FKBP5*, the T allele is linked to increased transcription and greater risk for psychiatric disorders and is therefore considered the risk allele. It has been proposed that these gene-environment interaction effects are mediated by the combined genetic and epigenetic changes that likely lead to even greater activation of *FKBP5* with GC and altered downstream effects on many relevant cellular pathways, including BDNF and dendritic spine density (Klengel et al., 2013; Matosin et al., 2018, 2023). It is thought that the CM-associated demethylation is driven by GCs. In fact, Wiechmann et al. (2019) described differential DNAm in several enhancers co-localizing with GR binding sites after acute administration of the GC agonist dexamethasone and this effect was moderated by the rs1360780 genotype. These sites overlapped in part with the ones previously found to be associated with CM, but extended well beyond them, as a more extensive fine-mapping approach was used (Roeh et al., 2018).

These studies provide first evidence that CM and GC exposure are linked to alterations in *FKBP5* DNAm and that these changes may be related to individual differences in stress-response brain networks and thus risk for disease (Kremer et al., 2024; Muehlhan et al., 2020; Tozzi et al., 2018). In a recent study for example, *FKBP5* demethylation in DNA from peripheral blood was related to an anxiety-associated reduction of gray matter volume in the ventromedial prefrontal cortex, a brain area that is involved in emotion regulation, mental health risk, and resilience as well as the responsivity of prefrontal-limbic circuits in relation to daily stressors (Kremer et al., 2024). This makes *FKBP5* DNAm in peripheral tissue an interesting biomarker candidate for stress-related psychiatric disease.

However, several important points have not been addressed by prior work: First, many existing studies on *FKBP5* DNAm and CM or psychiatric disease only inspect two specific CpGs in intron 7, and the choice of any additional CpGs on *FKBP5* is often driven by availability on DNAm microarrays rather than biological interest. It is very important to have sufficient coverage of CpGs in key regulatory regions, which is not always given when using array-based technologies (Wiechmann et al., 2019). For example, the effects of stress-related GC signaling on *FKBP5* transcription can be regulated via the demethylation of glucocorticoid-responsive elements (GREs), which are distributed across regions distal to the transcription start site, such as intronic enhancers (Paakinaho et al., 2010). Additionally, CTCF binding sites are present in the topologically associating domains (TADs) at the distal (3′) and proximal (5’) end of the gene, where they form architectural chromatin loops which facilitate interactions between promoter and enhancer (Wiechmann et al., 2019). The specific positions of GREs and CTCF binding sites are only sparsely featured on commercially available arrays. Thus, a more fine-grained approach to mapping epigenetic regulation across *FKBP5* is needed.

Second, DNAm patterns are cell type specific (Loyfer et al., 2023). Even between samples of the same tissues, cell type composition varies and leads to different DNAm signals. However, if no cell counts are available, cell type composition of samples can only be estimated from epigenome-wide measurements such as Illumina methylation microarrays. But epigenome-wide arrays and specific sequencing of *FKBP5* DNAm are rarely available simultaneously and many *FKBP5*-specific analyses have not taken cell type composition into account.

Third, DNAm is sensitive to a wide range of other pre-and postnatal exposures such as substance exposure in utero or maternal stress and depression (Maitre et al., 2022). These adverse exposures are also more common in unfavorable environments where postnatal CM is more likely to occur (Austin et al., 2022; Lebel et al., 2019). Therefore, prenatal exposures might be important confounders when assessing the effects of CM on DNAm. For example, epigenetic scores of prenatal cigarette smoke (Richmond et al., 2018) and alcohol exposure (Portales-Casamar et al., 2016) have previously been shown to be elevated in maltreated children (Martins et al., 2021) and are linked to worse developmental outcomes (Dufford et al., 2021).

Maternal psychiatric disorders and maternal stress exposure during pregnancy can be linked to altered brain structure (Mandl et al., 2024) and increased behavioral and emotional problems (Wu et al., 2022) in the offspring. Mechanistically, this may be related to increased exposure of the fetus to maternal circulating cortisol (Provençal and Binder, 2015). Increased prenatal exposure to synthetic GCs has been associated with offspring psychological and developmental disorders in several studies of antenatal corticosteroid treatment in women at risk of preterm birth (Ninan et al., 2022; Räikkönen et al., 2020, 2022).

Exposure to prenatal GCs also correlates with epigenetic changes: Placental *FKBP5* DNAm was shown to be lower in mothers who had been exposed to the synthetic GC betamethasone (Czamara et al., 2021). On an epigenome-wide level, Provençal et al. (2020) identified 496 CpGs that showed long-lasting methylation changes after dexamethasone treatment in a human hippocampal progenitor cell line as well as acute changes in human peripheral blood samples with the same treatment. The authors used these CpGs to construct an epigenetic score for glucocorticoid exposure via elastic net regression, selecting 24 CpGs that significantly predicted dexamethasone effects in human blood samples. The effects of dexamethasone treatment in human blood on DNA methylation were used to determine the weights for each CpG. The resulting epigenetic score (from here on referred to as the GC exposure score) was correlated with maternal depression and anxiety as well as prenatal synthetic GC exposure in cord blood samples, with lower methylation levels associated with higher exposure, suggesting that it may be an indicator of glucocorticoid exposure across tissues. In a further study, the GC exposure score was linked to worse mental health outcomes in mid-to-late childhood (Suarez et al., 2020). This makes the GC exposure score a potentially useful biomarker for tracking the epigenetic and biological impact of increased GC exposure. But as of yet, there is no integrative analysis linking CM to epigenetic alterations in *FKBP5* while considering the impact of prenatal exposures and of GC-responsive signaling across the epigenome.

To address these issues, we performed targeted bisulfite sequencing optimized for the *FKBP5* locus (HAM-TBS, Roeh et al., 2018) as well as epigenome-wide DNAm assessment using the Illumina EPICv1 arrays in saliva DNA samples at two repeated measurement times points in the Berlin Longitudinal Child Study. This is a cohort of children with (n = 83) and without maltreatment (n = 79), aged three to five years at baseline with extensive phenotyping and biological assessments (Winter et al., 2022). This allowed us better characterize *FKBP5* DNAm as a potential biomarker of risk by exploring the associations of CM with *FKBP5* DNAm in the context of prenatal exposures (as defined by DNAm exposure scores), variability in cell type composition, as well as endocrine and immune measures, and genotype.

2. Materials & methods

2.1. Study population

The Berlin Longitudinal Child Study (Berlin LCS) cohort (Dammering et al., 2021; Entringer et al., 2020; Joseph et al., 2023; Martins et al., 2021; Winter et al., 2022) consists of 173 children, aged 49 months on average (SD = 9.48) at the first visit. Maltreated children were recruited via child protection services and other help centers in the Berlin area. Non-maltreated children were recruited from the community.

As previously described (Winter et al., 2022), children who were exposed to maltreatment were identified by using the maltreatment classification system (MCS, Manly et al., 1994). The case definition criterion was exposure to at least one maltreatment event with sufficient severity. The severity of each maltreatment event was evaluated on a five-point scale ranging from mild (1) to severe or life-threatening maltreatment (5). Cut-offs of the scores were used to include children in the maltreatment group (emotional maltreatment ≥2, physical abuse ≥1, physical neglect ≥2). The control group included 87 children that had not been exposed to maltreatment as verified using the MMCI. Psychopathology and exposure to stressors and critical life events were assessed with the Preschool Age Psychiatric Assessment (PAPA, Egger and Angold, 2004). Information about parental mental disorders, preterm birth, and pregnancy complications was collected via self-report questionnaires filled out by the caregivers. Family socioeconomic status (SES) was assessed using a modified version of the Winkler and Stolzenberg Index (Lange et al., 2007).

From the baseline visit onwards, children were assessed every six months for two years with extensive psychometric and biological assessments. In addition, DNA from saliva samples was collected at five time points over the course of the study. In the study presented here, we used available saliva samples from baseline (T0, n = 162, maltreated = 83, controls = 79) as well as the one-year follow up time point (T2, n = 117, maltreated = 54, controls = 63). Demographics for participants at both time points are summarized in Table 1. While the sample was initially matched for age, sex, and maltreatment, the number of dropouts between T0 and T2 was higher among the maltreated group (33% in the maltreated group vs 21% in the non-maltreated group).

Approval for the study was obtained from the ethics committee of Charité – Universitätsmedizin Berlin. All procedures are in accordance with the Ethical Principles for Medical Research as established by the Medical Association Declaration of Helsinki. After the procedures were fully explained, written informed consent was obtained from all participants. Children gave consent by painting or signing a form that was appropriate for the children's age range. Caregivers received monetary compensation for participation and children received a small gift. Where required, caregivers received diagnostic results and referral for psychosocial or medical follow-up.

2.2. Saliva samples & biodata assays

As described in Entringer et al. (2020), during each clinical visit, saliva samples were collected via oral swabs which are specially designed for small children (Salimetrics) at 9am, 10am, and 11am. The samples were immediately stored at −80 °C. Genomic DNA was collected using ORAgene kits (OG-250 and OG-500, DNA Genotek) at the 9am timepoint. An automated and standardized procedure based on magnetic beads for 2× 400 μl saliva samples with the PerkinElmer Chemagic360 system was used for DNA extraction. Salivary C-reactive protein (CRP) was measured at one of the three timepoints using a commercial kit (Salimetrics) with a sensitivity of 10 pg/ml, intra-assay and inter-assay coefficients of variation of 6% and 13%. CRP data were log-transformed for further statistical analysis. Salivary cortisol was measured at all three timepoints on the day of assessment using a commercial ELISA kit (Salimetrics) with a sensitivity of 0.007 μg/dL. Intra-assay and inter-assay coefficients of variation were 7% and 11%, respectively. The area under the curve with respect to ground (AUCg) based on flow-rate corrected levels was chosen as the main cortisol readout since it was best correlated with baseline (9am, r = 0.59, p = $6.66*10^{-16}$) and peak (10am, r = 0.76, p < $2.2*10^{-26}$) cortisol levels. Cortisol outliers with >3 standard deviations from the mean were set to three standard deviations from the mean, which was the case for six samples.

Table 1
Demographics of the study population.

		Maltreated	Non-maltreated	p
Sample size	T0	83 (51.2%)	79 (48.8%)	/
	T2	54 (46.2%)	63 (53.8%)	/
Sex	T0	m = 44, f = 39	m = 41, f = 38	1.00
	T2	m = 28, f = 26	m = 32, f = 31	1.00
Mean age (years) ± SD	**T0**	**4.38 ± 0.84**	**4.08 ± 0.73**	**0.018**
	T2	**5.37 ± 0.84**	**5.07 ± 0.75**	**0.044**
Mean SES index ± SD	**T0**	**9.47 ± 4.52**	**16.04 ± 3.66**	**<0.001 ($<2.2*10^{-16}$)**
	T2	**9.46 ± 4.45**	**16.25 ± 3.65**	**<0.001 ($1.828*10^{-14}$)**
Any psychiatric diagnosis (%)	**T0**	**48 (57.8%)**	**15 (19.0%)**	**<0.001 ($9.198*10^{-07}$)**
	T2	**32 (59.3%)**	**9 (14.8%)**	**<0.001 ($1.771*10^{-06}$)**
Mean cortisol levels (AUCg) ± SD	T0	15.16 ± 0.84	12.84 ± 0.73	0.05
	T2	13.09 ± 0.84	14.21 ± 0.75	0.33
Mean CRP levels (AUCg) ± SD	T0	7.68 ± 0.83	7.60 ± 0.69	0.49
	T2	7.62 ± 0.82	7.54 ± 0.65	0.55
Mean proportion of CD34 cells	T0	33.92%	33.37%	0.41
	T2	**35.94%**	**34.08%**	**0.02**
Mean proportion of CD14 cells	T0	0.08%	0.13%	0.48
	T2	0.24%	0.16%	0.42
Mean proportion of buccal cells	T0	57.41%	58.28%	0.33
	T2	**54.78%**	**57.27%**	**0.007**
rs1360780 genotype (%)		**CT/TT (risk)**	**CC**	
	T0	78 (48.1%)	83 (51.2%)	0.94
	T2	54 (46.2%)	63 (53.8%)	0.34

Note. Maltreatment status (maltreated vs. non-maltreated) was assessed with the MCS (Manly et al., 1994). Psychiatric diagnosis (none vs. any) was determined using the PAPA (Egger and Angold, 2004). Socioeconomic status was assessed using the modified Winkler and Stolzenberg Index (Lange et al., 2007) and reflects low (score 3–8), middle (9–14), or high (15–21) family SES. Group differences between maltreated and non-maltreated children were tested via Fisher's exact tests or t-tests when appropriate. Nominally significant group differences are highlighted in bold.

2.3. DNAm data from the EPICv1 array

The Infinium MethylationEPIC v1.0 BeadChip (Illumina Inc) was used to measure DNA methylation, as described previously (Martins et al., 2021). Cell type proportions were estimated using the

deconvolution method described by Smith et al. (2015) and are shown in Table 1. These estimates obtained from DNAm patterns of the EPICv1 array were used to account for cell type proportions (buccal, CD14. and CD34 cells) in all statistical models in this study. CD34 is most commonly known as a marker for hematopoietic stem cells (Krause et al., 1996), which are unlikely to make up large parts of a saliva sample. We therefore also estimated cell type composition of our sample using a different reference panel for generic epithelial tissues by Zheng et al. (2018) that relies on the Houseman algorithm in the *EpiDISH* R package. Based on the Zheng panel, we identified proportions of 57.60–54.42% buccal cells (very similar to the proportion of buccal cells identified with the Smith panel), 42.20–45.22% immune cells, and 0.20–0.36% fibroblasts. The proportions of Zheng-based immune cells were strongly correlated with the Smith-based proportions of CD34 cells at T0 (Spearman correlation, rho = 0.86, p < 2.2–16) and T2 (Spearman correlation, rho = 0.77, p < 2.2–16). The correlations of estimated cell type proportions between the Smith and Zheng panels are depicted in Supplementary Fig. A1. Based on the correlation structure, the label "CD34" in this dataset is most likely a marker for diverse immune cells.

From the EPICv1 array data, we also computed epigenetic scores for prenatal tobacco exposure based on findings from Richmond et al. (2018) and prenatal alcohol exposure based on Portales-Casamar et al. (2016) as described in Martins (2022) to use as covariates in all statistical analyses. 13 out of the 15 original CpGs (86.77%) were available in the EPICv1 data for the smoke exposure score and 617 out of 658 CpGs (93.77%) were available for the alcohol exposure score. The prenatal smoke exposure score was validated in the Berlin LCS cohort in a previous publication, where it was significantly elevated in individuals with documented prenatal smoke exposure (Martins et al., 2021). Additionally, we computed the epigenetic GC exposure score from Provençal et al. (2020). 21 out of the 22 original CpGs (95.45%) were available in the current dataset. The original score only contains negative CpG weights and reflects hypomethylation upon GC exposure. Therefore, the score was multiplied with −1 for easier interpretation with a higher score denoting higher GC exposure.

2.4. Amplicon selection and targeted bisulfite sequencing of the FKBP5 locus

Targeted-bisulfite sequencing (HAM-TBS) is a method to measure methylation levels which is based on bisulfite conversion coupled with targeted enrichment via PCR, sequencing, and subsequent quantification. Targeted bisulfite sequencing of the *FKBP5* locus in the Berlin LCS samples was performed according to the procedure described by Roeh et al. (2018). Here, amplicons of 28 regions covering 302 CpGs within important regulatory sites, including GREs as well as CTCF binding sites and the transcription start site of the *FKBP5* locus had been optimized for HAM-TBS.

For this study, we selected eleven of these 28 amplicons covering regulatory regions of interest (*FKBP5* enhancers, intron 5, intron 7 as well as CTCF binding sites in the proximal 5′ and distal 3′TAD). Amplicons were selected to cover previously described GREs from Klengel et al. (2013) and the GR ChIP-Seq from the ENCODE project (The ENCODE Project Consortium, 2012). Additionally, amplicons covering CTCF binding sites were selected using HI-C peaks, CTCF-ChIA-Pet interactions from a lymphoblastoid cell line (GM12878, Tang et al., 2015), and CTCF ChIP-Seq information from the ENCODE project (Tang et al., 2015). Amplification failed for the PCR target *FKBP5* PCR 13.1 which was excluded from further analysis. The selected amplicons and the number of CpGs covered are described in Supplementary Table B1and their overlap with GREs and CTCF binding sites is depicted in Fig. 1.

Bisulfite treatment was performed on triplicates of each sample (3 × 50 ng) using the EZ DNA Methylation Kit (Zymo Research, Irvine, CA). Triplicates were then pooled to run one PCR amplification per amplicon, resulting in 150 ng of DNA used per sample. In the following, 1–5 μl of bisulfite-converted DNA were used for each PCR amplification employing Takara EpiTaq HS Polymerase (Clontech, Saint-Germain-en-Laye, France) with 49 amplification cycles. PCR amplicons were quantified with the Agilent 2200 TapeStation (Agilent Technologies, Waldbronn, Germany). The eleven different amplicons were then pooled in equimolar quantities for each sample. Primer dimers and high molecular DNA fragments were removed with AMPure XP beads (Beckman Coulter, Krefeld, Germany) using a double size selection (200–500 bp).

Libraries were prepared for each sample with the TruSeq DNA PCR-Free HT Library Prep Kit (Illumina, San Diego, CA) according to the manufacturer's instructions. Each library was quantified using the Qubit® 1.0 (Thermo Fisher Scientific Inc., Schwerte, Germany), then normalized to 4 nM and pooled. Library concentrations and fragment sizes were checked via Agilent's 2100 Bioanalyzer (Agilent Technologies, Waldbronn, Germany) and quantitative PCR using the Kapa HIFI Library quantification kit (Kapa Biosystems, Wilmington, MA). Paired-end (PE) sequencing was performed on an Illumina MiSeq Instrument (Illumina, San Diego, CA) using MiSeq Reagent Kit v3 (Illumina, San Diego, CA: 2 x 300 cycles) with the addition of 30% PhiX Library.

2.5. Processing of the sequencing data

The first step of quality control of the reads was performed using FastQC (Andrews et al., 2015). Adapter sequences were trimmed using Cupadapt (Martin, 2011). Reads were aligned against a bisulfite converted reference (Human GRCh37/hg19) restricted to the amplicon sequences using Bismark v0.18.2 (Krueger and Andrews, 2011). Paired-end reads were subsequently stitched with an in-house Perl script, which also removes low-quality tails of overlapping paired-end reads. Methylation levels for all CpGs, CHGs, and CHHs were quantified using the *methylKit* R package (Akalin et al., 2012). Quality control of the DNAm levels included the detection of PCR artefacts, the removal of samples with insufficient bisulfite conversion rate (<95%) as well as the exclusion of CpGs with coverage lower than 1000 reads. We were able to assess DNAm levels at 86% of the originally selected CpG sites after QC. The final dataset consisted of 49 CpGs from eleven amplicons in 162 samples (out of 165 original samples) at baseline and 117 samples (out of 120 original samples) at follow-up. All statistical analyses are based on beta values transformed to percentages (range = 0–100%). Mean DNAm levels for each of the covered CpGs are detailed in Supplementary Table B2.

2.6. Genotyping

Genotyping was performed with the Illumina GSA-24 v2.0 BeadChip as previously described (Martins et al., 2021). From this data, we used the genotype of rs1360780, a functional variant within the *FKBP5* locus, which has been widely studied in relation to stress reactivity, MDD, and PTSD (Binder et al., 2004; Kang et al., 2019; Klengel et al., 2013). The SNP did not deviate from Hardy-Weinberg-Equilibrium (p = 1) with observed genotype frequencies CC: 100, CT:80 and TT:16. Genotypes were grouped into CC and CT/TT for downstream analyses. As described in Martins et al. (2021), the first three genetic principal components explaining 35% of total genetic variance were extracted and used as covariates in subsequent analyses to adjust for population structure.

2.7. Statistical analysis

All statistical analyses were performed in R version 4.4.1 (R Core Team, 2023) and RStudio version 2024.04.2 + 764 (Posit team, 2024). In order to disentangle the contributions of individual predictors to variance in *FKBP5* DNAm, we performed a variance partitioning analysis via the *variancePartition* R package (Hoffman and Schadt, 2016). After excluding participants and CpGs with missing data, 39 CpGs from 149 individuals remained. Linear models including all available predictors (age, sex, CM, psychiatric diagnosis, SES, maternal psychopathology, pregnancy complications, stressful life events, genotype, cortisol and

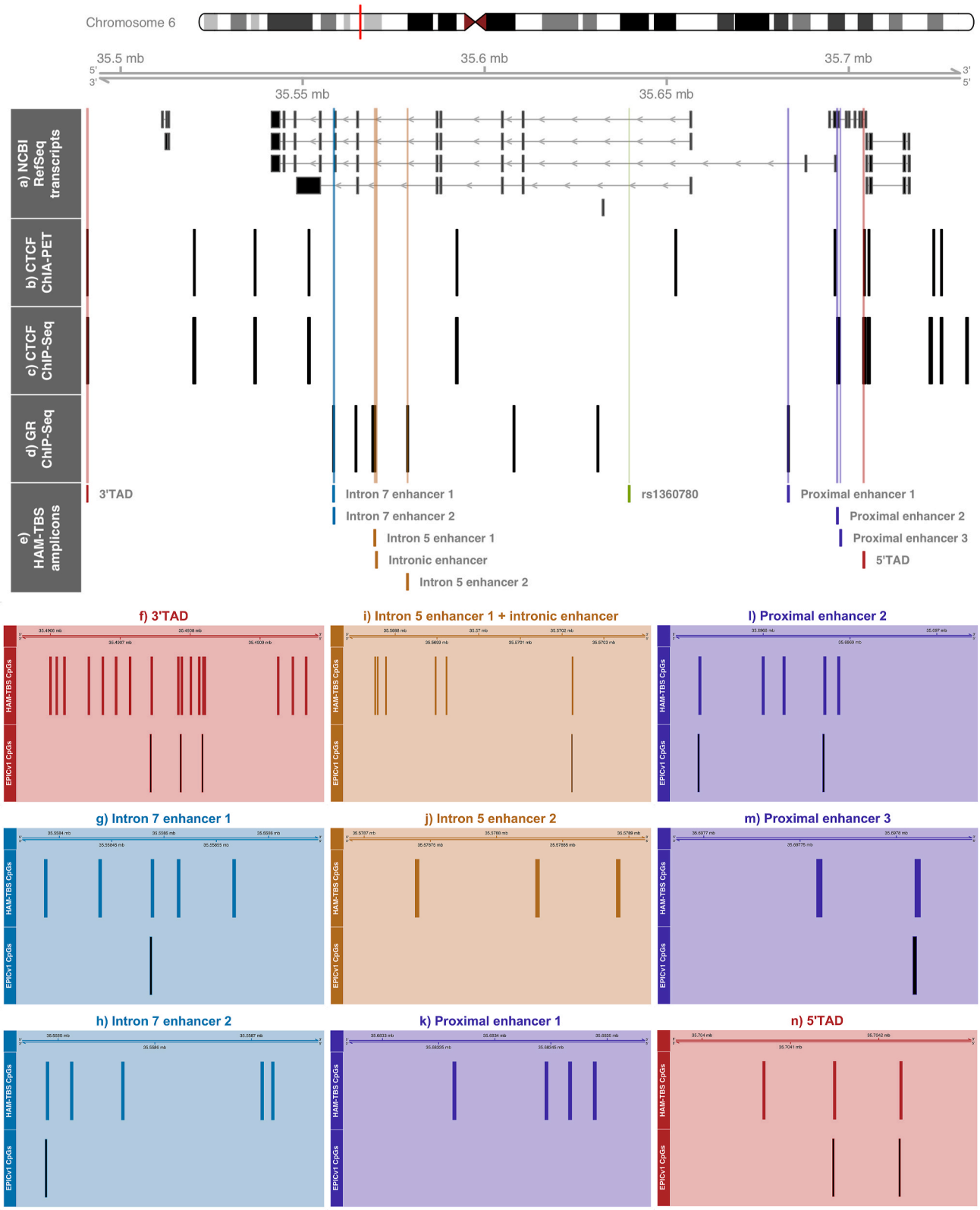

Fig. 1. Genomic locations of HAM-TBS amplicons.
Note. Genome browser view of *FKBP5*. Track a): transcripts located within the locus. Track b): locations of CTCF factor-mediated chromatin interactions (ChIA-PET data) extracted from lymphoblastoid cell line (GM12878, Tang et al., 2015). Track c) and d): transcription factor binding (CTCF & GR) obtained from chromatin immunoprecipitation (ChIP) experiments in multiple cell lines from the ENCODE project. Track e): positions of targeted bisulfite sequencing amplicons chosen for this project. Panels f) – n): exact positions of sequenced CpGs via HAM-TBS (top track) and via EPICv1 microarray (bottom track) per amplicon.

CRP levels, GC exposure score, prenatal smoking and alcohol exposure scores, estimated cell type proportions, and the first three genetic principal components), a time effect, and a random subject effect were run, returning the adjusted partial R^2 for each predictor and covariate per CpG.

To replicate previous effects from the literature (CM, psychiatric diagnosis, and genotype) on *FKBP5* DNAm, we ran linear regression models for each predictor of interest with methylation beta values per CpG as outcome. Raw p-values were corrected over all 49 CpGs using the Benjamini-Hochberg method (Benjamini and Hochberg, 1995) and the false-discovery rate (FDR) was set to 0.05. All regression models were adjusted for the following covariates: age, sex assigned at birth, the first three genetic principal components, estimated cell type proportions (CD34, CD14, and buccal), and epigenetic scores for prenatal exposure to cigarette smoke and alcohol, in line with previous analyses of the epigenome-wide data in this cohort (Martins et al., 2021). Age, sex, and the estimated cell type proportions were chosen as covariates since they have been shown to explain variance in DNA methylation in pediatric saliva samples (Middleton et al., 2022). The principal components were controlled for to adjust for ancestry and genetic effects on DNAm. Additionally, epigenetic scores predicting prenatal alcohol exposure and prenatal smoke exposure were added as covariates. These exposures are associated with altered DNAm patterns (Portales-Casamar et al., 2016; Richmond et al., 2018) and both exposure scores were significantly elevated in maltreated children in the Berlin LCS cohort (Martins et al., 2021), making them potential confounders. We also performed sensitivity analyses for the effects of CM where we added SES as an additional covariate to make sure that the CM effects were not due to SES differences between the maltreated and non-maltreated group.

Linear models were specified for each time point (T0 and T2). We also analyzed effects over time via ANOVA by comparing null models with a time effect to full models containing time and the predictor of interest. Additive interaction between CM and genotype was examined by testing whether adding genotype to the CM models significantly improved the model. Multiplicative interaction was tested by comparing a model with CM and genotype effects to a model containing a CM × genotype interaction term.

We then investigated effects of the epigenetic GC exposure score on *FKBP5* DNAm. We again used linear regression models with the GC exposure score as a predictor and the same outcomes and covariates as specified before. Additive and multiplicative interactions between genotype and GC exposure were analyzed as described previously for the CM-by-genotype effects. Next, we tested for associations of the GC exposure score with maternal mental disorder, self-reported pregnancy complications, maltreatment, psychopathology, and exposure to stressors and critical life events via linear regression models, correcting for the aforementioned covariates. P-values of the resulting twelve regression models were FDR-corrected for multiple testing.

Finally, we examined the correlation structure between estimated cell type proportions, the epigenetic exposure scores, cortisol, and CRP at both timepoints using Spearman correlations. We also computed Spearman correlations between the epigenetic exposure scores at both timepoints when residualized for the estimated cell type proportions.

3. Results

This study used a subset of children from the Berlin Longitudinal Child Study (Entringer et al., 2020) with available salivary DNA at baseline (T0, n = 162) and the one-year follow up (T2, n = 117). Age, SES, and the occurrence of psychiatric diagnoses differed significantly between maltreated and non-maltreated children at both timepoints, as depicted in Table 1. On average, the maltreated group was older, had lower SES, and more psychiatric diagnoses.

As described above, HAM-TBS amplicons were selected to cover GREs and CTCF binding sites within the *FKBP5* locus (see Fig. 1). We first performed a variance partitioning analysis to determine drivers of DNAm across functional regions of *FKBP5*, then aimed to replicate previous effects of CM and genotype, and further investigated associations of the GC exposure score with *FKBP5* DNAm, cortisol and CRP levels, and stress-related phenotypes.

3.1. Drivers of variability in FKBP5 DNAm

To gain more insight into drivers of variability in *FKBP5* DNAm, we included all available predictors into linear models over time, and summarized the percentage of variance (partial R^2) explained by each predictor for each CpG in Fig. 2. The total amounts of variance that could be explained by all predictors varied strongly from 6.15% in the proximal enhancer to 66.07% in the 3′TAD. Estimated cell type proportions explained the largest proportions of variance (0.14–34.20%), followed by DNAm-based scores of (prenatal) exposures (0.16–29.38%). The variance explained by cell type proportions was mostly driven by CD34 cells (0.02–16.99%) and buccal cells (0.02–16.71%), while CD14 cells only explained up to 1.41% of variance. Since the mean proportion of CD14 cells was smaller than 1% at both timepoints (see Table 1), their small contribution to *FKBP5* variability is expected. Among the epigenetic exposure scores, the GC exposure score explained the largest percentage of variance (0.001–28.28%), followed by prenatal alcohol exposure (0.001–6.06%) and prenatal smoke exposure (0.002–4.06%). The effects of cell type proportions and prenatal exposures were especially strong in the 3′TAD. In comparison, maltreatment explained a much smaller proportion of variance (0.00–2.48%), with most variance explained in CpGs located in the 5′ and 3′TAD and in the proximal enhancer.

3.2. Replication of previously reported associations

3.2.1. Association of maltreatment and psychopathology with FKBP5 DNAm

We first investigated differential DNAm between maltreated children (n = 83) and non-maltreated controls (n = 79). From the 49 CpGs covered by the HAM-TBS approach, nine CpGs showed nominally significant differential DNAm at baseline, but none of them survived FDR correction for multiple testing (see Supplementary Table B3). The uncorrected hits were distributed across the distal and proximal TAD, the proximal enhancer, intron 5, and intron 7, with the majority of hits located in intron 5 and the proximal enhancer. CpGs within intron 5 were hypermethylated in maltreated compared to non-maltreated children while the other functional regions were hypomethylated in maltreated children. Hypomethylation of *FKBP5* intron 7 has been associated with childhood adversity in multiple studies in both adults and children (e.g. Klengel et al., 2013; Parade et al., 2017; Tyrka et al., 2015), specifically in two CpGs (chr6:35558488 and chr6:35558514 on hg19). One of these CpGs (chr6:35558488) was also quantified in this project. While maltreated and non-maltreated children did not differ significantly here, this CpG was still hypomethylated in maltreated compared to non-maltreated children. In the present study, a different CpG in intron 7 (chr6:35558438) was nominally hypomethylated in children with CM. This site had also shown hypomethylation after exposure to the GC antagonist dexamethasone in adult peripheral blood samples (Wiechmann et al., 2019).

When investigating the effects of CM on *FKBP5* DNAm at the second timepoint one year later (T2), two CpGs in the distal 3'TAD were nominally hypermethylated in maltreated children, but did not survive FDR correction. There was no overlap between differentially methylated CpGs at T0 and T2. When fitting a linear model over time, eight CpGs showed nominally significant CM effects, six of them overlapping with the significant CpGs from T0. None of these CpGs remained significant after FDR correction. While the CM effects at T0 were distributed across all sequenced functional regions, the CM effects across time were restricted to the 3′TAD, proximal enhancer, and intron 5. Additional correction for SES did not alter the effects of CM on *FKBP5* DNAm to a

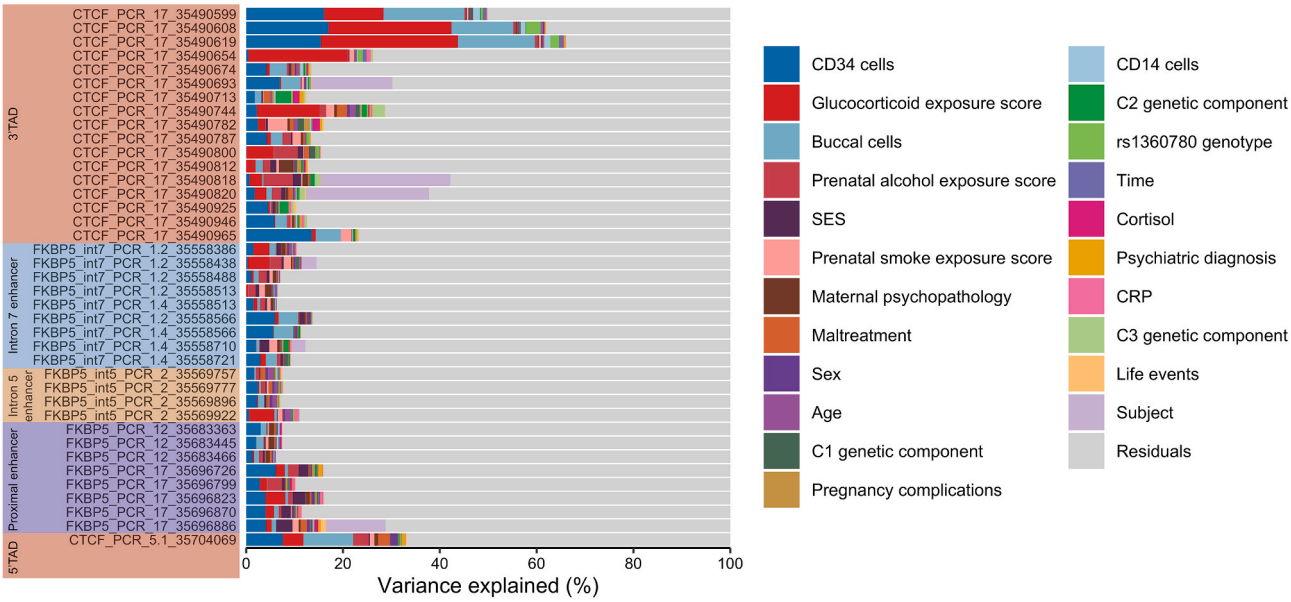

Fig. 2. Drivers of variance in *FKBP5* DNAm.
Note. Percentage of explained variance (partial R^2) for all predictors per sequenced position. The R^2 estimates result from linear regression models including all predictors, time, and a random subject effect to account for intra-individual variability from T0 to T2.

large degree. Most of the identified hits remained marginally significant when SES was added as a covariate. The results of the SES-controlled analyses are described in detail in **Appendix C**.

Next, we tested for differentially methylated CpGs between children with and without psychopathology (at least one diagnosis using the PAPA assessment). Again, no results survived multiple testing correction at either timepoint. Detailed results are available in Supplementary Table B4.

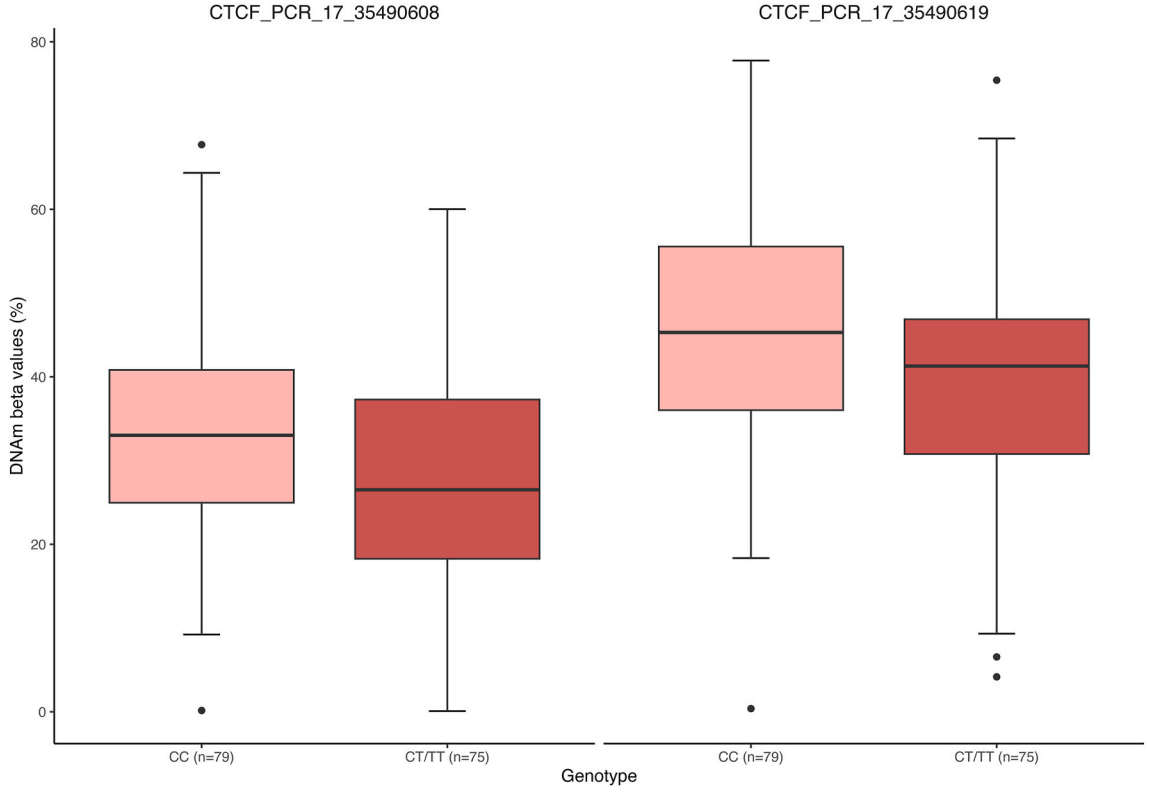

Fig. 3. Genotype-dependent CTCF binding site methylation.
Note. Two CpGs within the 3′TAD (chr6:35490608 and chr6:35490619) showed significantly lower methylation levels in carriers of the risk allele (CT/TT, shown in dark red) as compared to carriers of the protective genotype (CC, shown in pink). Both CpGs were highly correlated with $r = 0.83$ (Spearman correlation, $p < 2.2*10^{-16}$).

3.2.2. Association of SNP rs136780 with FKBP5 DNAm

We next tested for association of rs1360780 within the *FKBP5* locus with DNAm in functional regions of *FKBP5* at baseline. After multiple testing correction, two CpGs in the distal 3'TAD region remained significantly hypomethylated in carriers of the risk genotype (CT/TT), as visualized in Fig. 3. These two CpGs were located at positions chr6:3549608 (partial adj. $R^2 = 0.07$, adj. p = .030) and chr6:3549619 (partial adj. $R^2 = 0.06$, adj. p = .045). The CpG at chr6:3549608 was also nominally associated with CM in this study (see Supplementary Table B3). In the linear model fitted over time including T0 and T2, both significant CpGs from T0 were among the significant hits and survived FDR correction. Results are shown in Supplementary Table B5. Moreover, we tested for interaction effects of CM and genotype at T0, with no interaction passing multiple testing correction (see Supplementary Table B6). Nine CpGs in the TADs, intron 5 and 7, and the proximal enhancer showed nominally significant additive interaction effects at T0. All CpGs with additive interactions of rs1360780 genotype and CM overlapped with main effects of CM identified in section 3.2.1 (see Supplementary Table B3), including the previously discussed CpG in intron 7 (chr6:35558438). In the multiplicative interaction model, one CpG in the 3′TAD (chr6:35490800) and one CpG in the intron 5 intronic enhancer (chr6:35570224) showed marginally significant interaction effects of CM and genotype.

3.3. Glucocorticoid exposure

3.3.1. Association of the epigenetic GC exposure score with FKBP5 DNAm

The epigenetic GC exposure score showed three significant associations at T0 surviving FDR correction as detailed in Supplementary Table B7. All surviving hits were located in the 3′TAD at positions chr6:35490599 (partial adj. $R^2 = 0.09$, p (FDR) = 0.004), chr6:35490608 (partial adj. $R^2 = 0.12$, p (FDR) = 0.0004), and chr6:35490619 (partial adj. $R^2 = 0.12$, p (FDR) = 0.0005). All corrected significant hits from T0 were at least nominally significant and had the same direction of association at T2. The model fitted over time showed seven significant hits with four CpGs in the 3′TAD remaining significant post FDR correction, among them the surviving T0 hits. In all models, the majority of significant CpGs demonstrated consistent hypomethylation with increased predicted GC exposure.

When testing for additive interaction between rs1360780 genotype and glucocorticoid exposure, two CpGs survived FDR correction. Both additive hits were again located in the 3′TAD at positions chr6:35490608 (partial adj. R^2 GC exposure score = 0.13, partial adj. R^2 genotype = 0.08, p (FDR) = 0.025) and chr6:35490619 (partial adj. R^2 GC exposure score = 0.12, partial adj. R^2 genotype = 0.06, p (FDR) = 0.043) and overlapped with the significant main effects of genotype and GC exposure at T0. As depicted in Fig. 4, carrying the risk allele (CT/TT) as well as having a higher GC exposure score was associated with hypomethylation in the 3′TAD. Results at T2 are summarized in Supplementary Table B8. Multiplicative interaction models resulted in no significant results at T0 or T2.

3.3.2. Associations of the epigenetic GC exposure score with maternal and childhood phenotypes

In order to assess which other phenotypes track with the epigenetic GC exposure score, we tested for associations of GC exposure with maternal and childhood phenotypes (see Table 2) using the same covariates as in the *FKBP5* methylation models (age, sex, genetic principal components, estimated cell type proportions, prenatal alcohol exposure and prenatal smoke exposure scores). At T0, the score was associated with lifetime maternal mental disorders, self-reported pregnancy complications, and childhood maltreatment. Additionally, there were nominally significant associations with preterm birth at T0 and childhood maltreatment and maternal psychopathology at T2. In all

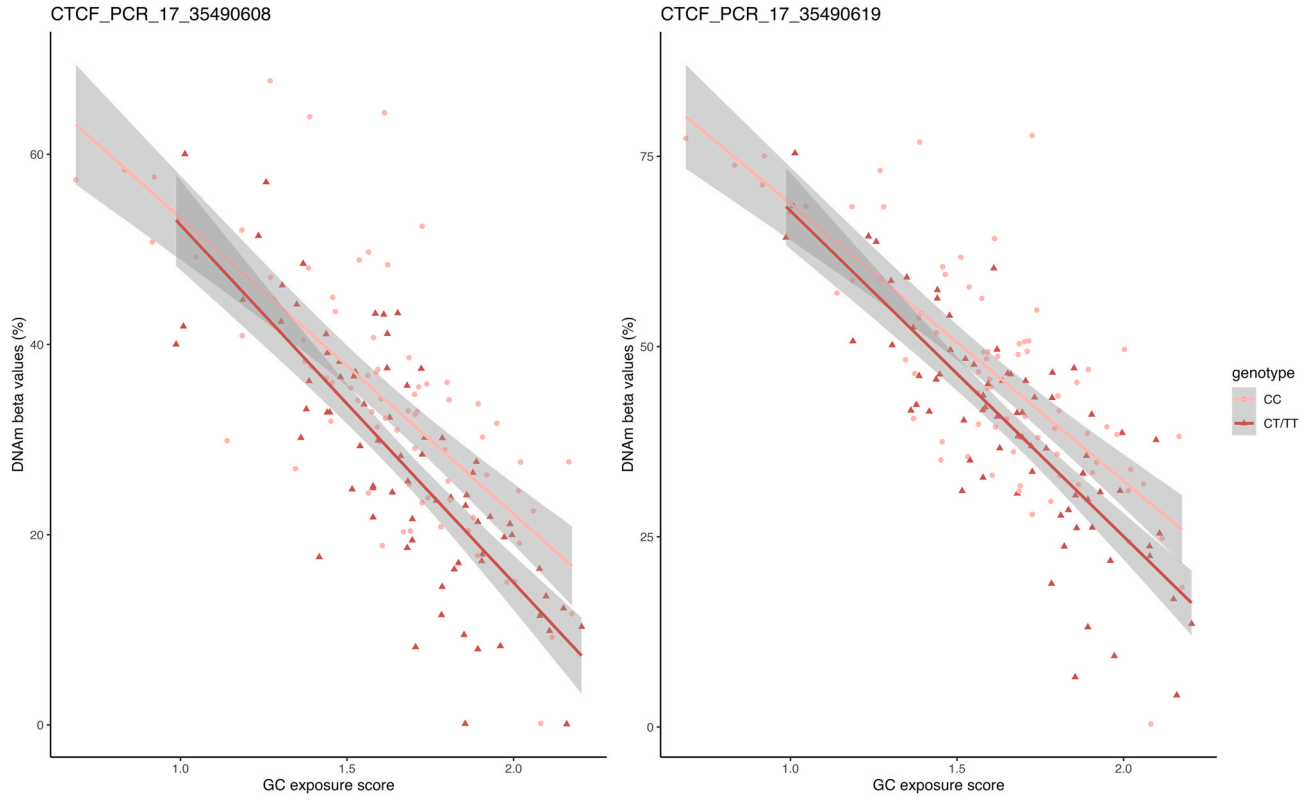

Fig. 4. Genotype-glucocorticoid interaction.
Note. FDR-corrected significant additive effects of GC exposure and rs1360780 genotype in the 3′TAD at T0. Carrying the risk allele (CT/TT, shown in dark red) and an increased GC exposure score were associated with hypomethylation.

Table 2
Associations of the glucocorticoid exposure score with maternal and child phenotypes at T0 and T2.

Phenotype	Time point	Beta	Adj. partial R^2	p	p (FDR)
Any maternal psychiatric diagnosis	T0	0.05	0.02	0.007	0.040
Any maternal psychiatric diagnosis	T2	0.06	0.09	0.020	0.060
Pregnancy complications	**T0**	**0.05**	**0.10**	**0.005**	**0.040**
Pregnancy complications	T2	0.01	0.03	0.784	0.947
Preterm birth	T0	0.05	0.08	0.039	0.084
Preterm birth	T2	0.00	−0.05	0.873	0.947
Maltreatment	**T0**	**0.04**	**0.04**	**0.011**	**0.044**
Maltreatment	T2	0.04	0.03	0.042	0.084
Any psychiatric diagnosis	T0	0.00	−0.01	0.917	0.947
Any psychiatric diagnosis	T2	0.03	0.00	0.137	0.205
Number of stressful life events	T0	0.00	−0.01	0.947	0.947
Number of stressful life events	T2	0.01	0.02	0.098	0.168

Note. Beta = beta coefficients of the main phenotype in the regression model, adj. partial R^2 = adjusted partial R^2 for predictor of interest, p = unadjusted p-values, p (FDR) = FDR-corrected p-values. FDR-corrected significant effects are highlighted in bold. All associations are based on linear regression models including age, sex, genetic principal components, estimated cell type proportions, prenatal smoke exposure, and prenatal alcohol exposure and are FDR-corrected for multiple testing over all 12 models. Maternal psychiatric diagnosis (none vs. any) was assessed via self-report questionnaires. The number of experienced stressful life events was assessed using the PAPA (Egger and Angold, 2004). Stressful life events included contextual stressors such as parental separation/divorce, parental arrest, or living in an unsafe neighborhood, and critical life events beyond CM such as having been hospitalized, having experienced the death of loved ones, or having been in a vehicular accident.

these, higher exposure levels were associated with higher predicted GC levels as indicated by positive betas. We detected no correlations with child psychopathology or exposure to stressful life events. Results are summarized in Table 2.

3.3.3. *Correlations of the epigenetic GC exposure score and biodata*

We further investigated the correlation structure between the epigenetic GC exposure score, epigenetic scores of prenatal smoking and alcohol exposure, estimated cell type proportions, saliva CRP, and cortisol using Spearman correlations (Fig. 5a). As expected, proportions of CD34 and buccal cells were strongly inversely correlated with each other (r = 0.92–0.95, p = $1.11*10^{-57}$- $5.37*10^{-52}$). CRP at T2 was correlated with the proportion of $CD14^{+}$ cells (r = 0.25, p = .01). Cortisol levels at T0 were significantly correlated with prenatal smoking (r = 0.23, p = .03) and alcohol exposure scores (r = 0.25, p = .04), but not with the GC exposure score (r = −0.19, p = .15), suggesting that this score indeed reflects past (prenatal) exposure and not current levels. The epigenetic exposure scores were significantly correlated with each other at the same timepoint, but only weakly correlated within individuals across timepoints. As soon as we corrected the epigenetic exposure scores for estimated cell type proportions, correlations between time-points became much higher (Fig. 5b), indicating that most time-point-dependent differences in the epigenetic exposure scores could likely be attributed to changes in cell type composition over time.

Notably, the GC exposure score was strongly *negatively* correlated with the epigenetic scores for prenatal alcohol and smoking exposure. However, all exposure scores were *positively* associated with CM status, as we have shown here for the GC exposure score (see Table 2) and as has also been demonstrated for alcohol and smoking exposure in Martins et al. (2021). The most likely explanation for this correlation structure is an interaction of CM and alcohol exposure on the GC exposure score. This is further explored in **Appendix D1** and Supplementary Figure D1. Potential reasons for this interaction pattern are discussed in detail in **Appendix D2**.

4. Discussion

FKBP5 DNAm in peripheral tissues may be a relevant biomarker of

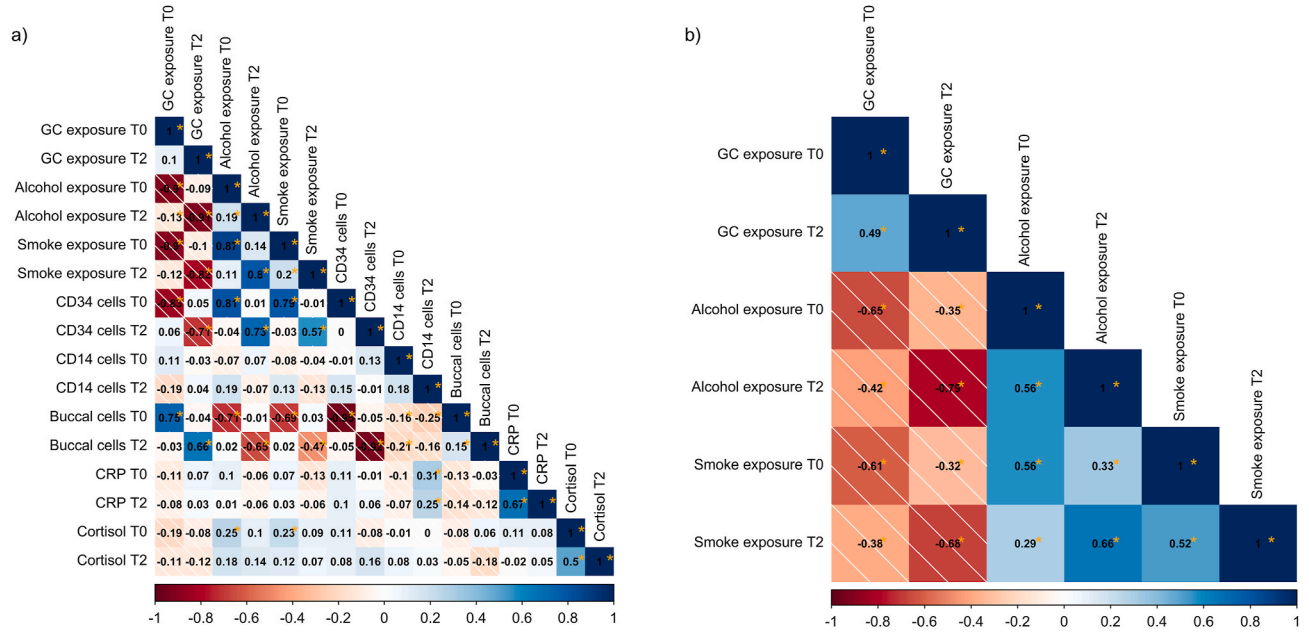

a) Correlation matrix of exposure scores, cell types, and biodata

b) Correlation matrix of exposure scores adjusted for cell type

Fig. 5. Correlation of exposure scores across timepoints.
Note. Panel a): Correlation matrix of epigenetic exposure scores, estimated cell type proportions, and biodata at T0 and T2. Panel b): Correlation matrix of epigenetic exposure scores residualized for estimated cell type proportions at T0 and T2. All depicted coefficients are Spearman correlations. Nominally significant correlations (uncorrected p < .05) are denoted with *.

risk following exposure to early life adversity (Kremer et al., 2024) and thus warrants detailed exploration of influencing factors. In the present study, we aimed to identify the main drivers of *FKBP5* DNAm in maltreated and non-maltreated children across 49 CpGs in regulatory regions of *FKBP5*, including proxies of prenatal exposures. We find that most variability of DNAm in saliva in this locus is explained by estimated cell type proportions as well as the epigenetic GC exposure score. CpG sites in the functionally relevant 3′TAD and upstream enhancers seem to be most influenced by the tested variables. These sites are not extensively covered in Illumina arrays, which demonstrates the benefits of fine mapping approaches. While not surviving correction for multiple testing, we replicate previously reported associations of *FKBP5* DNAm with CM. We also identify stable effects of rs1360780 genotype and the GC exposure score on DNAm in the 3′TAD. Our work again highlights the importance of assessing cell type heterogeneity in targeted assessments of DNAm and the need to document prenatal exposures or include epigenetic scores reflecting such exposures when investigating the effects of CM on DNAm.

4.1. Drivers of variance in FKBP5 DNAm

In a variance partitioning analysis, we first investigated the percentages of variance (partial R^2) explained by all available predictors ranging from cell types to prenatal exposures to maternal and child phenotypes. Estimated cell type proportions and DNAm-based scores of smoking, alcohol, and GC exposure emerged as major contributors to variance in *FKBP5* DNAm. Compared to that, much less variance was explained by CM and psychiatric diagnosis. These findings demonstrate that factors like estimated cell type proportions, which are usually seen as covariates or technical confounders, can have a much larger impact on DNAm than the actual effects of interest. Most studies either quantify DNAm via microarrays such as the EPIC BeadChip or via targeted sequencing of selected CpGs. It is rare to have both methods available simultaneously. This study shows that it is crucial to combine information from several epigenetic data modalities since estimated cell type proportions and epigenetic exposure scores, assessed using epigenome-wide DNAm arrays, also impact DNAm within specific candidate genes.

4.2. (Non-)replication of previous effects

We tested for effects of CM on *FKBP5* DNAm over 49 CpGs in different regulatory regions. While we were able to detect differences between maltreated and non-maltreated children in nine CpGs, none of the significant hits survived correction for multiple testing or remained significant at the second timepoint. However, several of the nominally significant CpGs at T0 were located in introns 5 and 7, the same regions that have shown CM effects in previous studies (Klengel et al., 2013; Parade et al., 2017; Tyrka et al., 2015; Wiechmann et al., 2019). Based on our sensitivity analyses, the nominally significant CM effects are unlikely to be confounded by differences in SES between maltreated and non-maltreated children. The methylation signature of psychopathology was similar, but not identical to that of CM, with three out of six nominally significant hits overlapping in the proximal enhancer at T0 and two out of three CpGs overlapping in the 3′TAD at T2. Further research is needed to fully disentangle the effects of adversity and symptomatology on *FKBP5* DNAm.

There are several possibilities why the CM effects on intron 7 methylation detected in Parade et al. (2017) and Tyrka et al. (2015) could not be replicated in this study, even though we also investigated saliva samples in a cohort of young children. First, this might be an issue of statistical power: Both Parade et al. (2017) and Tyrka et al. (2015) had larger sample sizes, but only tested two CpGs in intron 7, resulting in a much lower multiple testing burden. Moreover, our analyses were corrected for important potential confounders such as estimated cell type composition and prenatal exposure to smoking and alcohol, which have been linked to CM (Martins et al., 2021) and which have been shown to explain large amounts of variance in *FKBP5* DNAm in this study. Potentially, the effects of CM on saliva *FKBP5* DNAm are less apparent in a fine-mapping approach across several regulatory regions when proper statistical controls are considered.

While we were unable to fully replicate the effects of CM on *FKBP5* DNAm in intron 7, we observed *FKBP5* hypomethylation in rs1360780 risk allele carriers, as previously reported for adult blood samples in Klengel et al. (2013) and Wiechmann et al. (2019). Hence, this effect was stable across different tissues and age groups. The direct genotype effects were identified at CTCF binding sites the 3′TAD, a region at the distal end of *FKBP5*. Meanwhile, CM and rs1360780 genotype demonstrated marginally significant additive interaction effects in introns 5 and 7 where gene-environment interactions have also been observed by Klengel et al. (2013) and Wiechmann et al. (2019).

4.3. Glucocorticoid exposure

In this study, we examined the associations of a multi-tissue epigenetic score for GC exposure with both *FKBP5* DNAm and maternal and childhood phenotypes. To our knowledge, this score has not previously been investigated in relation to CM and *FKBP5* DNAm. We found that the GC exposure score explained up to 26% of variance in *FKBP5* DNAm, was strongly associated with hypomethylation of the 3′TAD, and displayed additive interaction with the rs1360780 genotype. Unlike effects of CM or psychopathology, the GC exposure effects were stable over time and survived correction for multiple testing. The large impact of the GC exposure score on *FKBP5* DNAm is especially interesting due to the role of the gene in HPA axis regulation: Prior research has shown that GC signaling induces *FKBP5* hypomethylation (Klengel et al., 2013; Wiechmann et al., 2019) which then increases *FKBP5* gene expression and alters regulation of the GC receptor.

To get a better picture on which stressors exactly correlate with the GC exposure score, we tested for associations of the score with maternal and childhood stressors. GC exposure was associated with maltreatment status and maternal psychopathology, but not with the number of experienced stressful life events and contextual stressors. There was also no correlation between the GC exposure score and current cortisol levels. Therefore, the score more likely reflects long-term effects of chronic stress exposure rather than an acute stress response. The score was additionally correlated with preterm birth and self-reported pregnancy complications, indicating that multiple “hits” can increase GC exposure in pre- and postnatal periods and replicating previous associations with prenatal factors (Provençal et al., 2020). Given that the GC score is associated with both CM and *FKBP5* DNAm, even though there are only few direct effects of CM on *FKBP5*, one might hypothesize that CM leads to increased GC exposure, which then in turn induces alterations in *FKBP5* DNAm. Consequently, the epigenetic GC exposure score might be a useful biomarker for tracking the effects of stress exposure on DNAm in further studies.

4.4. Biological relevance of the distal 3′TAD

The associations of rs1360780 and the GC exposure score with DNAm were only identified in the 3′TAD of *FKBP5*. This region is located at the very distal end of the gene and is usually not investigated in *FKBP5* DNAm studies, especially when targeted sequencing approaches are used. So, why were effects on DNAm observed specifically here? In general, TADs consist of CTCF binding sites which form architectural chromatin loops. Using 4C sequencing data, Wiechmann et al. (unpublished) have proposed a model of *FKBP5* TAD function: The structural loopings in the TAD aid the formation of promoter-enhancer interactions. Both GC stimulation and carrying the rs1360780 risk allele lead to the stabilization of chromatin loops in the TAD. This induces higher rates of interaction between enhancer and promoter, as well as more interaction between the proximal TAD and the gene body. As a consequence, more *FKBP5* mRNA is expressed. Given this model, it

makes sense that the GC exposure score and rs1360780 genotype showed individual and interaction effects specifically in this region. Our fine-mapping approach to quantifying *FKBP5* DNAm (HAM-TBS) covered 17 CpGs in the 3′TAD, while the Illumina EPICv1 microarray only covers three. Therefore, our sequencing approach provided better fine-mapping of a regulatory region that shows biological relevance for the effects of GC exposure. The distal 3′TAD of *FKBP5* remains a region of interest for further investigations.

4.5. Limitations

This study has several limitations: First, the sample size is limited with N = 162 at baseline. The sample size is even further reduced at the one-year follow-up (N = 117) with higher dropout rates among maltreated children. This means we are underpowered to detect smaller effects. In addition to larger samples, further follow-up measurements are necessary to assess the long-term effects of CM.

Second, many previous studies on *FKBP5* and CM have derived their results based on peripheral blood samples (e.g. Klengel et al., 2013; Wiechmann et al., 2019), while this investigation was performed on saliva samples. However, Smith et al. (2015) have investigated DNAm patterns across saliva, blood, and post-mortem brain samples and were able to demonstrate that saliva DNAm is more variable than blood or brain DNAm. It is therefore unclear how well this study's findings on drivers of *FKBP5* DNAm generalize to other tissues.

While the cell type composition of the saliva samples explained a large proportion of variance (0.14–34.20%) in this study, cell type proportions were not directly measured, but estimated from EPICv1 microarray data given a reference panel (Smith et al., 2015). Further studies, for example experimental work using sorted cells or single-cell quantification of DNAm, are needed to further disentangle cell type specific effects of CM on DNAm in *FKBP5* and beyond.

5. Conclusion

To summarize, this study identified estimated cell type proportions and prenatal exposures to cigarette smoke, alcohol, and glucocorticoids as the main drivers of DNAm across different functional regions of *FKBP5*. This emphasizes the relevance of considering epigenome-wide covariates even for candidate gene methylation studies. These findings also highlight the distal 3′TAD, a region not usually assessed in *FKBP5* studies, and underscore GC exposure as a potential link between early adversity and altered *FKBP5* DNAm. In conclusion, our results show the key importance of considering a wide range of exposures and adversities in DNAm studies: Not only maltreatment, but the entire early-life exposome affects DNAm and can steer individuals towards trajectories of health or disease.

CRediT authorship contribution statement

Vera N. Karlbauer: Writing – review & editing, Writing – original draft, Visualization, Formal analysis. **Jade Martins:** Writing – review & editing, Writing – original draft, Data curation. **Monika Rex-Haffner:** Resources, Investigation. **Susann Sauer:** Resources, Investigation. **Simone Roeh:** Resources, Methodology, Data curation. **Katja Dittrich:** Resources, Investigation. **Peggy Doerr:** Resources, Investigation. **Heiko Klawitter:** Resources, Investigation. **Sonja Entringer:** Supervision. **Claudia Buss:** Supervision, Investigation, Conceptualization. **Sibylle M. Winter:** Supervision, Resources, Investigation, Funding acquisition, Conceptualization. **Christine Heim:** Writing – review & editing, Supervision, Project administration, Funding acquisition, Conceptualization. **Darina Czamara:** Writing – review & editing, Supervision, Formal analysis, Data curation. **Elisabeth B. Binder:** Writing – review & editing, Supervision, Project administration, Funding acquisition, Conceptualization.

Code availability

R code for all statistical analyses is provided here: https://doi.org/10.5281/zenodo.13224255.

Funding

This study was funded by the German Federal Ministry of Education and Research (BMBF) 01KR1301-A (to CH) and 01KR1301-B and 01GL1743-C (to EBB). The research was conducted at Charite Universitaetsmedizin Berlin, Germany, and the Max Planck Institute of Psychiatry, Munich, Germany.

Declaration of competing interest

The authors declare the following financial interests/personal relationships which may be considered as potential competing interests: Elisabeth Binder has patent #FKBP5: a novel target for antidepressant therapy, European Patent #EP 1687443 B1 issued to the European Patent Office. The other authors declare that they have no known competing financial interests or personal relationships that could have appeared to influence the work reported in this paper.

Acknowledgements

We would like to thank the children and families who generously participated in this research.

Appendix A. Supplementary data

Supplementary data to this article can be found online at https://doi.org/10.1016/j.ynstr.2024.100687.

Data availability

Due to the sensitive nature of the data and consent, the Berlin LCS data are not publicly available. Interested researchers can obtain a deidentified dataset after approval from the study board.

References

Akalin, A., Kormaksson, M., Li, S., Garrett-Bakelman, F.E., Figueroa, M.E., Melnick, A., Mason, C.E., 2012. methylKit: A comprehensive R package for the analysis of genome-wide DNA methylation profiles. Genome Biol. 13 (10), R87. https://doi.org/10.1186/gb-2012-13-10-r87.

Aristizabal, M.J., Anreiter, I., Halldorsdottir, T., Odgers, C.L., McDade, T.W., Goldenberg, A., Mostafavi, S., Kobor, M.S., Binder, E.B., Sokolowski, M.B., O'Donnell, K.J., 2020. Biological embedding of experience: a primer on epigenetics. Proc. Natl. Acad. Sci. USA 117 (38), 23261–23269. https://doi.org/10.1073/pnas.1820838116.

Austin, A.E., Gest, C., Atkeson, A., Berkoff, M.C., Puls, H.T., Shanahan, M.E., 2022. Prenatal substance exposure and child maltreatment: a systematic review. Child. Maltreat. 27 (2), 290–315. https://doi.org/10.1177/1077559521990116.

Benjamini, Y., Hochberg, Y., 1995. Controlling the false discovery rate: a practical and powerful approach to multiple testing. J. Roy. Stat. Soc. B 57 (1), 289–300. https://doi.org/10.1111/j.2517-6161.1995.tb02031.x.

Binder, E.B., Salyakina, D., Lichtner, P., Wochnik, G.M., Ising, M., Pütz, B., Papiol, S., Seaman, S., Lucae, S., Kohli, M.A., Nickel, T., Künzel, H.E., Fuchs, B., Majer, M., Pfennig, A., Kern, N., Brunner, J., Modell, S., Baghai, T., et al., 2004. Polymorphisms in FKBP5 are associated with increased recurrence of depressive episodes and rapid response to antidepressant treatment. Nat. Genet. 36 (12), 1319–1325. https://doi.org/10.1038/ng1479.

Czamara, D., Dieckmann, L., Röh, S., Kraemer, S., Rancourt, R.C., Sammallahti, S., Kajantie, E., Laivuori, H., Eriksson, J.G., Räikkönen, K., Henrich, W., Plagemann, A., Binder, E.B., Braun, T., Entringer, S., 2021. Betamethasone administration during pregnancy is associated with placental epigenetic changes with implications for inflammation. Clin. Epigenet. 13 (1), 165. https://doi.org/10.1186/s13148-021-01153-y.

Dammering, F., Martins, J., Dittrich, K., Czamara, D., Rex-Haffner, M., Overfeld, J., de Punder, K., Buss, C., Entringer, S., Winter, S.M., Binder, E.B., Heim, C., 2021. The pediatric buccal epigenetic clock identifies significant ageing acceleration in children with internalizing disorder and maltreatment exposure. Neurobiology of Stress 15, 100394. https://doi.org/10.1016/j.ynstr.2021.100394.

Dufford, A.J., Spann, M., Scheinost, D., 2021. How prenatal exposures shape the infant brain: insights from infant neuroimaging studies. Neurosci. Biobehav. Rev. 131, 47–58. https://doi.org/10.1016/j.neubiorev.2021.09.017.

Egger, H., Angold, A., 2004. The Preschool Age Psychiatric Assessment (PAPA): a structured parent interview for diagnosing psychiatric disorders in preschool children. In: A Handbook of Infant and Toddler Mental Health Assessment. Oxford University Press.

Entringer, S., de Punder, K., Overfeld, J., Karaboycheva, G., Dittrich, K., Buss, C., Winter, S.M., Binder, E.B., Heim, C., 2020. Immediate and longitudinal effects of maltreatment on systemic inflammation in young children. Dev. Psychopathol. 32 (5), 1725–1731. https://doi.org/10.1017/S0954579420001686.

Hoffman, G.E., Schadt, E.E., 2016. variancePartition: interpreting drivers of variation in complex gene expression studies. BMC Bioinf. 17 (1), 483. https://doi.org/10.1186/s12859-016-1323-z.

Jiang, S., Postovit, L., Cattaneo, A., Binder, E.B., Aitchison, K.J., 2019. Epigenetic modifications in stress response genes associated with childhood trauma. Front. Psychiatr. 10. https://www.frontiersin.org/articles/10.3389/fpsyt.2019.00808.

Joseph, J., Buss, C., Knop, A., De Punder, K., Winter, S.M., Spors, B., Binder, E., Haynes, J.-D., Heim, C., 2023. Greater maltreatment severity is associated with smaller brain volume with implication for intellectual ability in young children. Neurobiology of Stress 27, 100576. https://doi.org/10.1016/j.ynstr.2023.100576.

Kang, J.I., Kim, T.Y., Choi, J.H., So, H.S., Kim, S.J., 2019. Allele-specific DNA methylation level of FKBP5 is associated with post-traumatic stress disorder. Psychoneuroendocrinology 103, 1–7. https://doi.org/10.1016/j.psyneuen.2018.12.226.

Klengel, T., Mehta, D., Anacker, C., Rex-Haffner, M., Pruessner, J.C., Pariante, C.M., Pace, T.W.W., Mercer, K.B., Mayberg, H.S., Bradley, B., Nemeroff, C.B., Holsboer, F., Heim, C.M., Ressler, K.J., Rein, T., Binder, E.B., 2013. Allele-specific FKBP5 DNA demethylation mediates gene-childhood trauma interactions. Nat. Neurosci. 16 (1), 33–41. https://doi.org/10.1038/nn.3275.

Klengel, T., Pape, J., Binder, E.B., Mehta, D., 2014. The role of DNA methylation in stress-related psychiatric disorders. Neuropharmacology 80, 115–132. https://doi.org/10.1016/j.neuropharm.2014.01.013.

Krause, D.S., Fackler, M.J., Civin, C.I., May, W.S., 1996. CD34: structure, biology, and clinical utility. Blood 87 (1), 1–13. https://doi.org/10.1182/blood.V87.1.1.1.

Kremer, T.L., Chen, J., Buhl, A., Berhe, O., Bilek, E., Geiger, L.S., Ma, R., Moessnang, C., Reichert, M., Reinhard, I., Schwarz, K., Schweiger, J.I., Streit, F., Witt, S.H., Zang, Z., Zhang, X., Nöthen, M.M., Rietschel, M., Ebner-Priemer, U.W., et al., 2024. Multimodal associations of FKBP5 methylation with emotion-regulatory brain circuits. Biol. Psychiatr. 0 (0). https://doi.org/10.1016/j.biopsych.2024.03.003.

Krueger, F., Andrews, S.R., 2011. Bismark: a flexible aligner and methylation caller for Bisulfite-Seq applications. Bioinformatics 27 (11), 1571–1572. https://doi.org/10.1093/bioinformatics/btr167.

Lange, M., Kamtsiuris, P., Lange, C., Schaffrath Rosario, A., Stolzenberg, H., Lampert, T., 2007. Messung soziodemographischer Merkmale im Kinder- und Jugendgesundheitssurvey (KiGGS) und ihre Bedeutung am Beispiel der Einschätzung des allgemeinen Gesundheitszustands. Bundesgesundheitsblatt - Gesundheitsforsch. - Gesundheitsschutz 50 (5–6), 578–589. https://doi.org/10.1007/s00103-007-0219-5.

Lebel, C.A., McMorris, C.A., Kar, P., Ritter, C., Andre, Q., Tortorelli, C., Gibbard, W.B., 2019. Characterizing adverse prenatal and postnatal experiences in children. Birth Defects Research 111 (12), 848–858. https://doi.org/10.1002/bdr2.1464.

Loyfer, N., Magenheim, J., Peretz, A., Cann, G., Bredno, J., Klochendler, A., Fox-Fisher, I., Shabi-Porat, S., Hecht, M., Pelet, T., Moss, J., Drawshy, Z., Amini, H., Moradi, P., Nagaraju, S., Bauman, D., Shveiky, D., Porat, S., Dior, U., et al., 2023. A DNA methylation atlas of normal human cell types. Nature 613 (7943). https://doi.org/10.1038/s41586-022-05580-6. Article 7943.

Maitre, L., Bustamante, M., Hernández-Ferrer, C., Thiel, D., Lau, C.-H.E., Siskos, A.P., Vives-Usano, M., Ruiz-Arenas, C., Pelegrí-Sisó, D., Robinson, O., Mason, D., Wright, J., Cadiou, S., Slama, R., Heude, B., Casas, M., Sunyer, J., Papadopoulou, E. Z., Gutzkow, K.B., et al., 2022. Multi-omics signatures of the human early life exposome. Nat. Commun. 13 (1), 7024. https://doi.org/10.1038/s41467-022-34422-2.

Mandl, S., Alexopoulos, J., Doering, S., Wildner, B., Seidl, R., Bartha-Doering, L., 2024. The effect of prenatal maternal distress on offspring brain development: a systematic review. Early Hum. Dev. 192, 106009. https://doi.org/10.1016/j.earlhumdev.2024.106009.

Manly, J.T., Cicchetti, D., Barnett, D., 1994. The impact of subtype, frequency, chronicity, and severity of child maltreatment on social competence and behavior problems. Dev. Psychopathol. 6 (1), 121–143. https://doi.org/10.1017/S0954579400005915.

Martin, M., 2011. Cutadapt removes adapter sequences from high-throughput sequencing reads. EMBnet.Journal 17 (1). https://doi.org/10.14806/ej.17.1.200. Article 1.

Martins, J., 2022. Multi-omics analysis of stress-related diseases [Technische Universität München]. https://mediatum.ub.tum.de/1625553.

Martins, J., Czamara, D., Sauer, S., Rex-Haffner, M., Dittrich, K., Dörr, P., de Punder, K., Overfeld, J., Knop, A., Dammering, F., Entringer, S., Winter, S.M., Buss, C., Heim, C., Binder, E.B., 2021. Childhood adversity correlates with stable changes in DNA methylation trajectories in children and converges with epigenetic signatures of prenatal stress. Neurobiology of Stress 15. https://doi.org/10.1016/j.ynstr.2021.100336.

Matosin, N., Arloth, J., Czamara, D., Edmond, K.Z., Maitra, M., Fröhlich, A.S., Martinelli, S., Kaul, D., Bartlett, R., Curry, A.R., Gassen, N.C., Hafner, K., Müller, N. S., Worf, K., Rehawi, G., Nagy, C., Halldorsdottir, T., Cruceanu, C., Gagliardi, M., et al., 2023. Associations of psychiatric disease and ageing with FKBP5 expression converge on superficial layer neurons of the neocortex. Acta Neuropathol. 145 (4), 439–459. https://doi.org/10.1007/s00401-023-02541-9.

Matosin, N., Halldorsdottir, T., Binder, E.B., 2018. Understanding the molecular mechanisms underpinning gene by environment interactions in psychiatric disorders: the FKBP5 model. Biol. Psychiatr. 83 (10), 821–830. https://doi.org/10.1016/j.biopsych.2018.01.021.

Middleton, L.Y.M., Dou, J., Fisher, J., Heiss, J.A., Nguyen, V.K., Just, A.C., Faul, J., Ware, E.B., Mitchell, C., Colacino, J.A., Bakulski, K.M., 2022. Saliva cell type DNA methylation reference panel for epidemiological studies in children. Epigenetics 17 (2), 161–177. https://doi.org/10.1080/15592294.2021.1890874.

Muehlhan, M., Miller, R., Strehle, J., Smolka, M.N., Alexander, N., 2020. FKBP5 methylation predicts functional network architecture of the rostral anterior cingulate cortex. Brain Struct. Funct. 225 (1), 33–43. https://doi.org/10.1007/s00429-019-01980-z.

Ninan, K., Liyanage, S.K., Murphy, K.E., Asztalos, E.V., McDonald, S.D., 2022. Evaluation of long-term outcomes associated with preterm exposure to antenatal corticosteroids: a systematic review and meta-analysis. JAMA Pediatr. 176 (6), e220483. https://doi.org/10.1001/jamapediatrics.2022.0483.

Normann, C., Buttenschøn, H.N., 2020. Gene–environment interactions between HPA-axis genes and childhood maltreatment in depression: a systematic review. Acta Neuropsychiatr. 32 (3), 111–121. https://doi.org/10.1017/neu.2020.1.

Paakinaho, V., Makkonen, H., Jääskeläinen, T., Palvimo, J.J., 2010. Glucocorticoid receptor activates poised FKBP51 locus through long-distance interactions. Mol. Endocrinol. 24 (3), 511–525. https://doi.org/10.1210/me.2009-0443.

Parade, S.H., Huffhines, L., Daniels, T.E., Stroud, L.R., Nugent, N.R., Tyrka, A.R., 2021. A systematic review of childhood maltreatment and DNA methylation: candidate gene and epigenome-wide approaches. Transl. Psychiatry 11 (1), 134. https://doi.org/10.1038/s41398-021-01207-y.

Parade, S.H., Parent, J., Rabemananjara, K., Seifer, R., Marsit, C.J., Yang, B.-Z., Zhang, H., Tyrka, A.R., 2017. Change in FK506 binding protein 5 (*FKBP5*) methylation over time among preschoolers with adversity. Dev. Psychopathol. 29 (5), 1627–1634. https://doi.org/10.1017/S0954579417001286.

Portales-Casamar, E., Lussier, A.A., Jones, M.J., MacIsaac, J.L., Edgar, R.D., Mah, S.M., Barhdadi, A., Provost, S., Lemieux-Perreault, L.-P., Cynader, M.S., Chudley, A.E., Dubé, M.-P., Reynolds, J.N., Pavlidis, P., Kobor, M.S., 2016. DNA methylation signature of human fetal alcohol spectrum disorder. Epigenet. Chromatin 9 (1), 25. https://doi.org/10.1186/s13072-016-0074-4.

Posit team, 2024. *RStudio: Integrated Development Environment For R* (Version 2024.04.2+764) [Computer Software]. Posit Software, PBC. http://www.posit.co/.

Provençal, N., Arloth, J., Cattaneo, A., Anacker, C., Cattane, N., Wiechmann, T., Röh, S., Ködel, M., Klengel, T., Czamara, D., Müller, N.S., Lahti, J., Räikkönen, K., Pariante, C.M., Binder, E.B., Kajantie, E., Hämäläinen, E., Villa, P., Laivuori, H., 2020. Glucocorticoid exposure during hippocampal neurogenesis primes future stress response by inducing changes in DNA methylation. Proc. Natl. Acad. Sci. USA 117 (38), 23280–23285. https://doi.org/10.1073/pnas.1820842116.

Provençal, N., Binder, E.B., 2015. The effects of early life stress on the epigenome: from the womb to adulthood and even before. Exp. Neurol. 268, 10–20. https://doi.org/10.1016/j.expneurol.2014.09.001.

R Core Team, 2023. R: A Language and Environment for Statistical Computing (Version 4.4.1) [Computer Software]. R Foundation for Statistical Computing. https://www.R-project.org/.

Räikkönen, K., Gissler, M., Kajantie, E., 2020. Associations between maternal antenatal corticosteroid treatment and mental and behavioral disorders in children. JAMA 323 (19), 1924–1933. https://doi.org/10.1001/jama.2020.3937.

Räikkönen, K., Gissler, M., Tapiainen, T., Kajantie, E., 2022. Associations between maternal antenatal corticosteroid treatment and psychological developmental and neurosensory disorders in children. JAMA Netw. Open 5 (8), e2228518. https://doi.org/10.1001/jamanetworkopen.2022.28518.

Richmond, R.C., Suderman, M., Langdon, R., Relton, C.L., Davey Smith, G., 2018. DNA methylation as a marker for prenatal smoke exposure in adults. Int. J. Epidemiol. 47 (4), 1120–1130. https://doi.org/10.1093/ije/dyy091.

Roeh, S., Wiechmann, T., Sauer, S., Ködel, M., Binder, E.B., Provençal, N., 2018. HAM-TBS: high-accuracy methylation measurements via targeted bisulfite sequencing. Epigenet. Chromatin 11 (1), 1–10. https://doi.org/10.1186/s13072-018-0209-x.

Smith, A.K., Kilaru, V., Klengel, T., Mercer, K.B., Bradley, B., Conneely, K.N., Ressler, K. J., Binder, E.B., 2015. DNA extracted from saliva for methylation studies of psychiatric traits: evidence tissue specificity and relatedness to brain. Am. J. Med. Genet. Part B: Neuropsychiatric Genetics 168 (1), 36–44. https://doi.org/10.1002/ajmg.b.32278.

Suarez, A., Lahti, J., Lahti-Pulkkinen, M., Girchenko, P., Czamara, D., Arloth, J., Malmberg, A.L.K., Hämäläinen, E., Kajantie, E., Laivuori, H., Villa, P.M., Reynolds, R.M., Provençal, N., Binder, E.B., Räikkönen, K., 2020. A polyepigenetic glucocorticoid exposure score at birth and childhood mental and behavioral disorders. Neurobiology of Stress 13, 100275. https://doi.org/10.1016/j.ynstr.2020.100275.

Tang, Z., Luo, O.J., Li, X., Zheng, M., Zhu, J.J., Szalaj, P., Trzaskoma, P., Magalska, A., Wlodarczyk, J., Ruszczycki, B., Michalski, P., Piecuch, E., Wang, P., Wang, D., Tian, S.Z., Penrad-Mobayed, M., Sachs, L.M., Ruan, X., Wei, C.-L., et al., 2015. CTCF-mediated human 3D genome architecture reveals chromatin topology for transcription. Cell 163 (7), 1611–1627. https://doi.org/10.1016/j.cell.2015.11.024.

The ENCODE Project Consortium, 2012. An integrated encyclopedia of DNA elements in the human genome. Nature 489 (7414), 57–74. https://doi.org/10.1038/nature11247.

Tozzi, L., Farrell, C., Booij, L., Doolin, K., Nemoda, Z., Szyf, M., Pomares, F.B., Chiarella, J., O'Keane, V., Frodl, T., 2018. Epigenetic changes of FKBP5 as a link connecting genetic and environmental risk factors with structural and functional

brain changes in major depression. Neuropsychopharmacology 43 (5), 1138–1145. https://doi.org/10.1038/npp.2017.290.

Tyrka, A.R., Ridout, K.K., Parade, S.H., Paquette, A., Marsit, C.J., Seifer, R., 2015. Childhood maltreatment and methylation of FK506 binding protein 5 gene (*FKBP5*). Dev. Psychopathol. 27 (4pt2), 1637–1645. https://doi.org/10.1017/S0954579415000991.

Wiechmann, T., Röh, S., Sauer, S., Czamara, D., Arloth, J., Ködel, M., Beintner, M., Knop, L., Menke, A., Binder, E.B., Provençal, N., 2019. Identification of dynamic glucocorticoid-induced methylation changes at the FKBP5 locus. Clin. Epigenet. 11 (1), 83. https://doi.org/10.1186/s13148-019-0682-5.

Winter, S.M., Dittrich, K., Dörr, P., Overfeld, J., Moebus, I., Murray, E., Karaboycheva, G., Zimmermann, C., Knop, A., Voelkle, M., Entringer, S., Buss, C., Haynes, J.D., Binder, E.B., Heim, C., 2022. Immediate impact of child maltreatment on mental, developmental, and physical health trajectories. J. Child Psychol. Psychiatry Allied Discip. https://doi.org/10.1111/jcpp.13550.

Wu, Y., Espinosa, K.M., Barnett, S.D., Kapse, A., Quistorff, J.L., Lopez, C., Andescavage, N., Pradhan, S., Lu, Y.-C., Kapse, K., Henderson, D., Vezina, G., Wessel, D., du Plessis, A.J., Limperopoulos, C., 2022. Association of elevated maternal psychological distress, altered fetal brain, and offspring cognitive and social-emotional outcomes at 18 months. JAMA Netw. Open 5 (4), e229244. https://doi.org/10.1001/jamanetworkopen.2022.9244.

Zannas, A.S., Arloth, J., Carrillo-Roa, T., Iurato, S., Röh, S., Ressler, K.J., Nemeroff, C.B., Smith, A.K., Bradley, B., Heim, C., Menke, A., Lange, J.F., Brückl, T., Ising, M., Wray, N.R., Erhardt, A., Binder, E.B., Mehta, D., 2015. Lifetime stress accelerates epigenetic aging in an urban, African American cohort: relevance of glucocorticoid signaling. Genome Biol. 16 (1), 1–12. https://doi.org/10.1186/s13059-015-0828-5.

Zheng, S.C., Webster, A.P., Dong, D., Feber, A., Graham, D.G., Sullivan, R., Jevons, S., Lovat, L.B., Beck, S., Widschwendter, M., Teschendorff, A.E., 2018. A novel cell-type deconvolution algorithm reveals substantial contamination by immune cells in saliva, buccal and cervix. Epigenomics 10 (7), 925–940. https://doi.org/10.2217/epi-2018-0037.